A Scalable Var Planning Methodology to Mitigate Reactive Power Scarcity During Energy Transition

Elnaz Davoodi, *Member, IEEE*, Florin Capitanescu, *Senior Member, IEEE*, Mohammad Iman Alizadeh, *Member, IEEE*, Louis Wehenkel

Abstract—The paper re-thinks the reactive power (or Var) planning problem to mitigate reactive power scarcity in the prevailing context of the energy transition to renewable-dominated power supply. The paper first proposes an enhanced tailored problem formulation of Var planning, in the form of a stochastic multi-period AC security-constrained optimal power flow; it minimizes the investment cost in new reactive power assets to meet power system constraints under various operating conditions. Then, the paper develops a new scalable methodology to solve this Var planning problem; it achieves scalability by a progressive and efficient identification of the binding combinations of contingencies, time periods, and uncertainty scenarios, which allows solving sequentially problems of much smaller size than the original one. The performance of the methodology is demonstrated on a 60-bus model of the Nordic system and a 1203-bus model of a real system.

Index Terms—energy transition, reactive power scarcity, security-constrained optimal power flow, Var planning

NOMENCLATURE

Notation: vectors and matrices are written in **bold** characters.

A. Acronyms

DA	Direct approach
MINLP	Mixed-integer nonlinear programming
RES	Renewable energy sources
SC	Synchronous condenser
S-MP-SCOPF	Stochastic multi-period AC security-constrained optimal power flow
STATCOM	Static synchronous compensator
SVC	Static Var compensator
WPP	Wind power plant
TSO	Transmission system operator

B. Subscripts

c	Capacitor
d	Load demand
g	Synchronous generator
pv	Photovoltaic solar farm
r	Reactor
sc	Synchronous condenser

scm	Static synchronous compensator
sh	Existing shunt element (capacitor/reactor)
svc	Static Var compensator
wp	Wind power plant

C. Sets

$\mathcal{C}$	Set of the potential nodes to install capacitors
$\mathcal{K}$	Set of system states (indexed by k): normal operation ($k = 0$) or after a contingency ($k \geq 1$)
$\mathcal{L}^k$	Set of branches (lines and transformers) in state k
$\mathcal{N}$	Set of nodes (or buses), indexed by i
$\mathcal{O}$	Set of transformers with controllable ratio
$\mathcal{P}$	Set of time periods, indexed by p
$\mathcal{PV}$	Set of photovoltaic solar farms
$\mathcal{R}$	Set of the potential nodes to install reactors
$\mathcal{S}$	Set of RES uncertainty scenarios, indexed by s
$\mathcal{SC}$	Set of the potential nodes to install SCs
$\mathcal{SCM}$	Set of the potential nodes to install STATCOMs
$\mathcal{SH}$	Set of existing shunt elements (capacitors/reactors)
$\mathcal{SVC}$	Set of the potential nodes to install SVCs
$\mathcal{T}_{r/v/s}$	Set of relevant/violated/selected tuples
$\mathcal{W}$	Set of wind power plants

D. Parameters

$c_{\text{r/c/sc/svc/scm}}$	Capital investment cost coefficients of the reactor, capacitor, SC, SVC, and STATCOM
$I_{ij}^{\max}$	Maximal current of the branch ij
$I_{gi}^{\max}$	Maximum stator current of the generator at bus i
P_{di}	Active power load demand at bus i
$P_{\text{pv}i}$	Solar active power generation at bus i
$P_{\text{wp}i}$	Active power generation of WPP at bus i
Q_{di}	Reactive power load demand at bus i
$Q_{gi}^{\max}$	Maximum reactive power of the generator at bus i
$Q_{gi}^{\min}$	Minimum reactive power of the generator at bus i
$Q_{\text{sc}i}^{\max}$	Maximum reactive power of the SC at bus i
$Q_{\text{sc}i}^{\min}$	Minimum reactive power of the SC at bus i
$Q_{\text{wp}i}^{\max}$	Maximum reactive power of the WPP at bus i
$Q_{\text{wp}i}^{\min}$	Minimum reactive power of the WPP at bus i
$V_{\text{f}i}^{\max}$	Maximum field induced voltage of generator at bus i

E. Continuous decision variables ($\forall\ k \in \mathcal{K}, \forall\ s \in \mathcal{S}, \forall\ p \in \mathcal{P}$)

$b_{\text{sh}i}^{k,s,p}$	Susceptance of the existing shunt element at bus i
$b_{\text{svc}i}^{k,s,p}$	Susceptance of SVC at bus i
$b_{\text{svc}i}^{\max}$	Maximum susceptance of the SVC at bus i

$I_{\text{scm}i}^{k,s,p}$ Reactive current of STATCOM at bus i

$I_{\text{scm}i}^{\max}$ Maximum reactive current of the STATCOM at bus i

$P_{\text{g}i}^{k,s,p}$ Active power of the synchronous generator at bus i

$Q_{\text{g}i}^{k,s,p}$ Reactive power of the synchronous generator at bus i

$Q_{\text{sc}i}^{k,s,p}$ Reactive power of the SC at bus i

$Q_{\text{sc}i}^{k,s,p}$ Maximum reactive power of the SC at bus i

$Q_{\text{wp}i}^{k,s,p}$ Reactive power of WPP at bus i

$t_{ij}^{k,s,p}$ Ratio of the transformer between buses i and j

$V_{\text{c}i}^{k,s,p}$ Controllable voltage (e.g. by SVC, SCs) at bus i

F. Discrete decision variables ($\forall\ k \in \mathcal{K}, \forall\ s \in \mathcal{S}, \forall\ p \in \mathcal{P}$)

$b_{\text{c}i}^{k,s,p}$ Susceptance of the capacitor at bus i

$b_{\text{c}i}^{\max}$ Maximum susceptance of the capacitor at bus i

$b_{\text{r}i}^{k,s,p}$ Susceptance of the reactor at bus i

$b_{\text{r}i}^{\max}$ Maximum susceptance of the reactor at bus i

G. Continuous state variables ($\forall\ k \in \mathcal{K}, \forall\ s \in \mathcal{S}, \forall\ p \in \mathcal{P}$)

$\theta_i^{k,s,p}$ Voltage phase angle at bus i

$V_i^{k,s,p}$ Voltage magnitude at bus i

I. INTRODUCTION

To combat climate change, power systems are transitioning to 100% low-carbon or renewable energy supply. During this energy transition, valuable sources of reactive power, i.e. fossil fuel-based conventional generators, will be progressively phased out and replaced by a myriad of RES. Such massive system transformation poses multiple challenges to grid operation security in various respects: low inertia, power balancing, voltage control, and protection.

This work is concerned with voltage issues. In this respect, the location, size, and quality of the grid Var support are undermined by the retirement of conventional synchronous generators and deployment of RES, resulting in uncoordinated, ad-hoc Var support which is far from optimal. Indeed, RES are non-optimally located to support voltages because they are: (i) scattered at all voltage levels, including distribution networks, that are not under the control of the TSO, (ii) deployed to exploit climatic conditions (e.g. off-shore wind power) but are ineffective for voltage control in critical areas since reactive power does not travel far. In addition, in terms of the quality (capability range) of Var support, inverter-based RES are inferior to conventional generators [1].

In this context, it is envisioned that power systems are going to face alarming situations of lack or excess of reactive power, which weaken the voltage control capability leading to under-voltages, over-voltages and frequent voltage fluctuations outside the statutory limits [2]. In response to the fast pace of the energy transition, utilities need to react to preserve grid security. To this end, TSOs should dispose of methods to identify when reactive power becomes scarce [1] and then, to mitigate emerging voltage issues, develop a Var planning coordinated approach that best exploits existing and new Var capabilities in the grid.

Reactive power (or Var) planning problem consists of minimizing the investment cost in new reactive power sources (e.g. capacitors, reactors, SCs) during a certain time horizon to ensure voltage security (i.e. voltages can be controlled within their limits in normal operation and after contingencies) in the transmission grid [3]. Accordingly, the Var planning problem determines the optimal location, size, and type of reactive power sources to be installed along with their sequence of deployment.

Clearly, the Var planning problem must be rethought in the prevailing transmission grid operation context. However, solving the problem is highly challenging even today due to: 1) the large size, stemming from the consideration of $N - 1$ contingencies, 2) nonlinearity and nonconvexity of grid operation model, and 3) discreteness of some reactive power sources (e.g. capacitors, reactors). Hence, Var planning is a large-scale MINLP problem, which is out of the reach of the existing off-the-shelf solvers and requires tailoring a scalable solution approach.

Given the pivotal role of reactive power in unexpected blackouts [4], various approaches have been proposed to the Var planning problem. These differ in terms of (i) the model of objectives and/or constraints, and (ii) solution approaches, each exhibiting unique mathematical and computational characteristics [3].

Early Var planning methods use linearization [5] due to its advantages such as dependable performance, flexibility to model diverse power system operating limits, and the ability to detect infeasibility. However, linear methods generally lack precision and often fail to generate exact solutions to the highly nonlinear relationship between voltage and reactive power.

To improve accuracy, subsequently, approaches such as successive quadratic programming [6] and Newton's method [7] have been investigated, requiring the computation of second-order partial derivatives of power-flow equations and other constraints. To further tackle discrete variables, methods such as Benders decomposition [8], branch and bound [9], successive MILP approximation [10], or penalty functions in successive conic programming [11] have ben applied. Finally, meta-heuristic algorithms have also been used [12]; they are straightforward to implement but lack mathematical guarantees on feasibility and optimality and are not scalable.

The previously mentioned studies take a deterministic approach to Var planning without considering the impact of RES, the energy transition, or reactive power scarcity. A distinct advantage of the proposed methodology is that identifying scarcity by the approach proposed in [1] serves as a foundation for informing crucial aspects of the Var planning problem, such as the timing and location of new reactive power sources.

Recently, a few works have considered in various ways RES and to some extent the energy transition perspective, as follows. Ref. [13] computes, for a small system, the size of reactive power sources but only under a limited number of scenarios of RES uncertainty and critical contingencies. Ref. [14] proposes a multi-stage coordinated approach for planning capacitors and STATCOMs to enhance voltage resilience in a wind energy power system. Ref. [15] develops a many-objective robust dynamic Var planning method for wind energy power systems aiming to improve steady-state and short-term voltage stability. Ref. [16] presents a probabilistic AC-DC load flow method, incorporating the connection between offshore wind farms and the grid, for planning capacitors and SVCs. Lastly, Ref. [17] proposes a bi-level optimization technique, based on

a multi-objective genetic algorithm, to optimally allocate Var sources and select optimal locations for wind farms to enhance voltage stability.

The review of the state-of-the-art in Var planning allows inferring that some shortcomings persist: a) absence of a scalable approach to large-scale MINLP problems typical for real-world power systems, b) limited modeling depth of static or dynamic Var sources as well as narrow options of Var assets for TSOs to make informed decisions, c) inadequate exploration of the effects of corrective control actions, d) simplified models of synchronous generators' reactive power capability, and e) insufficient attention to accurately estimate the timing for Var planning during the energy transition. This work addresses these shortcomings.

In other words, the previous works have addressed only partly the challenges and complexity of the Var planning problem needed in the future in terms of problem features and scalable solution approach. This paper significantly extends our preliminary work in [18], its unique contributions being the following:

- new necessary features that refine and enhance the realism of the problem formulation, namely: scenarios modeling RES uncertainty, time aspects, accurate modeling of reactive power capability of conventional generators and WPP, and a comprehensive array of dynamic and static Var assets. In addition, to make the problem formulation comprehensive, the discreteness of decision variables is jointly considered.
- a novel tailored tractable solution methodology that loops among: smaller size versions of the S-MP-SCOPF problem, treatment of discrete variables, steady-state security assessment, and selection of relevant combinations of contingencies, time periods, and uncertainty scenarios.

Note that scalable methodologies to solve specific large-scale MINLP AC SCOPF problems[1] exist [21]–[23]. However, the proposed methodologies (e.g. [21]–[23]) require significant adaptation work to be applied to the proposed Var problem.

II. THE PROPOSED VAR PLANNING PROBLEM

This section elaborates on the proposed tailored S-MP-SCOPF formulation of the Var planning problem. The latter should be solved before reactive power shortage creates voltage issues during the energy transition. To this end, we build upon our previous work in [1], which unveils the point where reactive power becomes scarce and informs it as input to the proposed methodology.

A key peculiarity of the Var planning is that Var assets can be deployed in the field possibly from a few months to 2 years. Therefore, the Var planning problem adopts a time horizon of 1-2 years ahead and is performed in a single stage. The Var planning problem can be resolved for subsequent future time horizons by updating the system state and development plans.

The problem models the yearly system operation considering:

- a certain number of time periods $p \in \mathcal{P}$ (e.g. $|\mathcal{P}| = 24$)[3] for some selected representative days, e.g. combinations of day types based on the season (spring, summer, autumn, winter) and the week day (weekday, weekend);
- a certain number of scenarios $s \in \mathcal{S}$ modeling RES real power uncertainty.

A. Objective function

The Var planning problem minimizes the capital investment cost in new Var assets, dynamic (SVCs, STATCOMs, SCs) and static (reactors, capacitors), to be installed at selected locations:

$$\min_{\substack{\mathbf{P}_{\mathrm{g}},\mathbf{V}_{\mathrm{c}},\mathbf{Q}_{\mathrm{g}},\mathbf{Q}_{\mathrm{wp}},\mathbf{Q}_{\mathrm{sc}}, \\ \mathbf{t},\mathbf{b}_{\mathrm{r/c/svc}},\mathbf{I}_{\mathrm{scm}}, \\ \mathbf{Q}_{\mathrm{sc}}^{\max},\mathbf{b}_{\mathrm{r/c/svc/scm}}^{\max}}} \sum_{i \in \mathcal{R}} c_{\mathrm{r}i} \cdot b_{\mathrm{r}i}^{\max} + \sum_{i \in \mathcal{C}} c_{\mathrm{c}i} \cdot b_{\mathrm{c}i}^{\max}$$
$$+ \sum_{i \in \mathcal{SC}} c_{\mathrm{sc}i} \cdot Q_{\mathrm{sc}i}^{\max} + \sum_{i \in \mathcal{SVC}} c_{\mathrm{svc}i} \cdot b_{\mathrm{svc}i}^{\max} \qquad (1)$$
$$+ \sum_{i \in \mathcal{SCM}} c_{\mathrm{scm}i} \cdot I_{\mathrm{scm}i}^{\max}$$

Note that as the discrete sizes of Var assets can take the value zero, there is no need to introduce a supplementary binary variable to model whether an asset is deployed or not at a bus.

The model differences of the Var assets are as follows. The reactive power of SCs varies continuously within physical limits similar to the synchronous generators. Var assets such as capacitors, reactors, and SVCs behave as variable susceptance, see (2)–(4), while the STATCOM behaves as variable reactive current (5):

$$Q_{\mathrm{r}i}^{k,s,p}(b_{\mathrm{r}i}^{k,s,p}, V_i^{k,s,p}) = -b_{\mathrm{r}i}^{k,s,p}\left(V_i^{k,s,p}\right)^2, \quad \forall i \in \mathcal{R} \qquad (2)$$

$$Q_{\mathrm{c}i}^{k,s,p}(b_{\mathrm{c}i}^{k,s,p}, V_i^{k,s,p}) = b_{\mathrm{c}i}^{k,s,p}\left(V_i^{k,s,p}\right)^2, \quad \forall i \in \mathcal{C} \qquad (3)$$

$$Q_{\mathrm{svc}i}^{k,s,p}(b_{\mathrm{svc}i}^{k,s,p}, V_i^{k,s,p}) = b_{\mathrm{svc}i}^{k,s,p}\left(V_i^{k,s,p}\right)^2, \quad \forall i \in \mathcal{SVC} \qquad (4)$$

$$Q_{\mathrm{scm}i}^{k,s,p}(I_{\mathrm{scm}i}^{k,s,p}, V_i^{k,s,p}) = I_{\mathrm{scm}i}^{k,s,p} V_i^{k,s,p}, \quad \forall i \in \mathcal{SCM} \qquad (5)$$

Further, the susceptance of SVCs varies continuously while the susceptance of reactors/capacitors varies in discrete steps.

The STATCOM fulfils the same role as the SVC but has two advantages in operation [24]. First, once STATCOM upper reactive power limit is reached, it generates a larger amount of reactive power than the SVC as it behaves as a constant current (hence its reactive power diminishes linearly with the bus voltage) while the SVC behaves as constant susceptance (hence the reactive power varies with the square of the bus voltage). Second, STATCOM has several ms faster response to faults in the absence of thyristor firing delay of SVC.

Note that the TSO may pre-select locations that require the deployment of Var assets with continuous voltage regulation (SC, SVC, STATCOM) due to factors such as the risk of voltage instability or voltage fluctuations, including both limits violation, due to RES variability. Such operating conditions require fast and steady voltage control that cannot be met by capacitors/reactors, which are cheaper but have slower responses and their reactive power depends on the square of the voltage.

The objective does not include the benefits of installing new Var assets in reducing the operation cost (e.g. decrease of power losses and the cost of re-dispatch to meet voltage limits) as this cost is negligible as compared to the assets' capital investment.

B. Operation Constraints

The baseline formulation adopts the widely-used *preventive security mode* [25], which states that decision variables (of Var assets) cannot change after a contingency (23). The rationale of it is that, after a contingency occurs, the operator may not have the necessary time to estimate the system state, optimize it, and broadcast new setpoints to Var assets. Section II-C presents the problem extension to a hybrid *preventive-corrective* mode [26].

The operation constraints apply $\forall:\ k \in \mathcal{K},\ s \in \mathcal{S},\ p \in \mathcal{P}$.

$$P_{gi}^{k,s,p} + P_{wpi}^{s,p} + P_{pvi}^{s,p} - P_{di}^{p} = P_i^{k,s,p}(\mathbf{V}, \boldsymbol{\theta}, \mathbf{t}), \forall i \in \mathcal{N} \tag{6}$$

$$Q_{gi}^{k,s,p} + Q_{wpi}^{k,s,p} + Q_{sci}^{k,s,p} + (V_i^{k,s,p})^2 (b_{shi}^{k,s,p} + b_{ci}^{k,s,p} - b_{ri}^{k,s,p}$$
$$+ b_{svci}^{k,s,p}) + V_i^{k,s,p} I_{scmi}^{k,s,p} - Q_{di}^{p} = Q_i^{k,s,p}(\mathbf{V}, \boldsymbol{\theta}, \mathbf{t}), \quad \forall i \in \mathcal{N} \tag{7}$$

$$b_{shi}^{min} \le b_{shi}^{k,s,p} \le b_{shi}^{max}, \qquad \forall i \in \mathcal{SH} \tag{8}$$

$$0 \le b_{ri}^{k,s,p} \le b_{ri}^{max}, \qquad \forall i \in \mathcal{R} \tag{9}$$

$$0 \le b_{ci}^{k,s,p} \le b_{ci}^{max}, \qquad \forall i \in \mathcal{C} \tag{10}$$

$$- b_{svci}^{max} \le b_{svci}^{k,s,p} \le b_{svci}^{max}, \qquad \forall i \in \mathcal{SVC} \tag{11}$$

$$- b_{scmi}^{max} V_i^{k,s,p} \le I_{scmi}^{k,s,p} \le b_{scmi}^{max} V_i^{k,s,p}, \forall i \in \mathcal{SCM} \tag{12}$$

$$- Q_{sci}^{max} \le Q_{sci}^{k,s,p} \le Q_{sci}^{max}, \qquad \forall i \in \mathcal{SC} \tag{13}$$

$$P_{gi}^{min} \le P_{gi}^{k,s,p} \le P_{gi}^{max}, \qquad i = \{slack\} \tag{14}$$

$$P_{gi}^{k,s,p} = P_{gi,imp}^{s,p,0}, \qquad \forall i \in \mathcal{G} \setminus \{slack\} \tag{15}$$

$$Q_{gi}^{min} \le Q_{gi}^{k,s,p} \le Q_{gi}^{max}, \qquad \forall i \in \mathcal{G} \tag{16}$$

$$Q_{wpi}^{min} \le Q_{wpi}^{k,s,p} \le Q_{wpi}^{max}, \qquad \forall i \in \mathcal{W} \tag{17}$$

$$I_{ij}^{k,s,p}(\mathbf{V}, \boldsymbol{\theta}, \mathbf{t}) \le I_{ij}^{max}, \qquad \forall (i,j) \in \mathcal{L}^k \tag{18}$$

$$t_{ij}^{min} \le t_{ij}^{k,s,p} \le t_{ij}^{max}, \qquad \forall (i,j) \in \mathcal{O} \tag{19}$$

$$V_i^{min} \le V_{ci}^{k,s,p} \le V_i^{max}, \forall i \in \{\mathcal{G} \cup \mathcal{SC} \cup \mathcal{SVC} \cup \mathcal{SCM}\} \tag{20}$$

$$V_i^{min} \le V_i^{k,s,p} \le V_i^{max}, \forall i \in \mathcal{N} \setminus \{\mathcal{G} \cup \mathcal{SC} \cup \mathcal{SVC} \cup \mathcal{SCM}\} \tag{21}$$

$$\theta_i^{k,s,p} = 0, \qquad i = \{slack\} \tag{22}$$

$$\mathbf{z}^{k\ge1,s,p} = \mathbf{z}^{k=0,s,p}, \qquad \mathbf{z} \equiv \{\mathbf{V}_c, \mathbf{Q}_{wp}, \mathbf{b}_{sh}, \mathbf{b}_r, \mathbf{b}_c, \mathbf{t}\} \tag{23}$$

Equality constraints (6)–(7) represent the nodal active and reactive power balance considering the impact of new reactive power sources wherein $P_i^{k,s,p}(.)$ and $Q_i^{k,s,p}(.)$ define the net injected active and reactive power flow into bus i.

The physical limits on the capacity of existing and new Var sources are defined in (8)–(13). The deployment decision of Var sources and their size are managed by the decision variables $b_{r/c/svci}^{max}$, which may take the value zero (i.e. no deployment) and are independent of time, scenario, and state.

Equation (14) constrains the active power of the "slack" generator assumed. For the sake of simplicity, the slack generator is solely responsible for balancing real power mismatch in each combination of the time period, scenario, and system state.

Constraint (15) indicates that the active power output of all generators except the slack generator is fixed at the imposed value $P_{gi,imp}^{s,p,0}$; this is a typical assumption in reactive power dispatch problems as active power has a much larger cost and is deemed already dispatched at the lowest cost. Accordingly, the

generators' active power is not re-dispatched to minimize the investment cost in Var sources. Instead, we assume that optimal generators' dispatch for different time periods and scenarios, i.e. $P_{gi,imp}^{s,p,0}$, stems from active power electricity market clearing and is an input to the Var planning problem.

Constraints (16) and (17) guarantee that the reactive power of synchronous generators and WPPs stay within the physical range, respectively.

Constraint (18) models the thermal limit of the network lines $\forall (i,j) \in \mathcal{L}^k$. Constraints (19) limit the transformers' ratio. Equation (20) imposes limits on voltage magnitudes at voltage-controllable nodes. Equation (21) establishes bounds on the voltage magnitudes at buses without voltage control assets. Constraint (22) sets the angle reference.

Constraints (23) define the *preventive mode* constraints, which impose that the controlled voltage (of generators, SCs, SVCs, and STATCOMs), reactive power of WPPs, the susceptance (of existing shunt elements, reactors, and capacitors), and transformers controllable ratios are state-independent.

The mathematical model (1)-(23) forms the base proposed MINLP formulation of the S-MP-SCOPF Var planning problem.

Two further model refinements are elaborated hereafter.

C. Problem Extension to Hybrid Preventive-Corrective Mode

The preventive mode (23) does not allow to re-dispatch control means, excepting automated control, in response to contingencies. However, if the system possesses assets that can be actuated fast, the TSO may be able to adjust them within their limits to mitigate voltage issues after a contingency [26].

Accordingly, this work implements separately both *preventive*, see (23), and *preventive-corrective* modes, see (24)–(25).

The mathematical model of the Var planning problem in hybrid preventive-corrective mode is hence (1)-(22), (24)-(25).

$$V_{ci}^{k\ge1,s,p} = V_{ci}^{k=0,s,p}, \quad \forall i \in \{\mathcal{G} \cup \mathcal{SC} \cup \mathcal{SVC} \cup \mathcal{SCM}\} \tag{24}$$

$$|\mathbf{z}'^{k\ge1,s,p} - \mathbf{z}'^{k=0,s,p}| \le \Delta \mathbf{z}', \quad \mathbf{z}' \equiv \{\mathbf{b}_{sh}, \mathbf{b}_r, \mathbf{b}_c, \mathbf{t}\} \tag{25}$$

Constraints (24) reflect the current industrial practice, where each generator needs to keep its voltage constant in any state.

D. Refinements of Reactive Power Limits

For a precise modeling of synchronous generators and WPPs reactive power capability in VAr planning, constant reactive power limit in (16)-(17) are insufficient. The proposed enhanced representation of their reactive power capabilities is outlined in equations (26), (27), and (28) [27], [28].

$$(Q_{gi}^{max})^{k,s,p} = \min \left\{ \begin{array}{l} \sqrt{\left(\frac{V_i^{k,s,p} V_{fi}^{max}}{x_{gi}}\right)^2 - (P_{gi}^{k,s,p})^2} - \frac{(V_i^{k,s,p})^2}{x_{gi}}, \\ \sqrt{(V_i^{k,s,p} I_{gi}^{max})^2 - (P_{gi}^{k,s,p})^2} \end{array} \right. \tag{26}$$

$$(Q_{wpi}^{max})^{s,p} = \min \left\{ (Q_{V,wpi}^{max})^{s,p}, (Q_{I,wpi}^{max})^{s,p} \right\} + b_{wpi}\left(V_{mvi}\right)^2 \tag{27}$$

$$(Q_{wpi}^{min})^{s,p} = \max \left\{ (Q_{V,wpi}^{min})^{s,p}, Q_{I,wpi}^{min})^{s,p} \right\} + b_{wpi}\left(V_{mvi}\right)^2 \tag{28}$$

Equation (26), enforces limitations on the field and armature winding heating of synchronous generators, where $V_\mathrm{f}^\mathrm{max}$, x_g, and $I_\mathrm{g}^\mathrm{max}$ represent the maximum field voltage, synchronous reactance, and maximum stator current, respectively. For converter-based WPPs, specifically type 4 wind turbines, the reactive power capability can be expressed through (27)–(30). In these equations, $Q_{V,\mathrm{wp}}$ and $Q_{I,\mathrm{wp}}$ represent the reactive power capability of WPPs constrained by the voltage and current of the grid-side converter, respectively. Furthermore, $z_\mathrm{wp} = r_\mathrm{wp} + j x_\mathrm{wp}$ signifies the combined impedance of wind turbines and the WPP collection system, while V_co and I_co indicate the magnitude of voltage and current for the grid-side converters of the WPPs. Additionally, $V_{\mathrm{mv}i}$ stands for the medium voltage of the WPP transformer, and b_wp models the equivalent shunt susceptance of the WPP collection system.

In (30), the positive and negative roots correspond to the maximum production and absorption capacity of the WPP. To determine the maximum injection and absorption of reactive power limited by converter voltage in (29), the converter voltage ($V_\mathrm{co}^{k,s,p}$) is replaced by the maximal ($V_\mathrm{co}^\mathrm{max}$) and minimum ($V_\mathrm{co}^\mathrm{min}$) allowable converter voltage, respectively. Similarly, to calculate the bounds of reactive power limited by the converter current, the converter current $I_\mathrm{co}^{k,s,p}$ in (30) is replaced by the maximum allowable converter current $I_\mathrm{co}^\mathrm{max}$. Constraints (27) and (28) further consider the reactive power injected by cables due to the equivalent WPP collection system susceptance; it is added to the maximum injection and absorption capability obtained at the medium voltage side of the transformer.

$$Q_{V,\mathrm{wp}i}^{k,s,p} = \sqrt{\left(\frac{V_{\mathrm{mv}i}V_{\mathrm{co}i}^{k,s,p}}{|z_{\mathrm{wp}i}|}\right)^2 - \left(P_{\mathrm{wp}i}^{s,p} + \frac{(V_{\mathrm{mv}i})^2 r_{\mathrm{wp}i}}{|z_{\mathrm{wp}i}|^2}\right)^2}$$
$$- \frac{(V_{\mathrm{mv}i})^2 x_{\mathrm{wp}i}}{|z_{\mathrm{wp}i}|^2} \qquad (29)$$

$$Q_{I,\mathrm{wp}i}^{k,s,p} = \pm\sqrt{\left(V_{\mathrm{mv}i}I_{\mathrm{co}i}^{k,s,p}\right)^2 - (P_{\mathrm{wp}i}^{s,p})^2} \qquad (30)$$

III. The Proposed Solution Methodology

A. Aim, Rationale, and Main Steps

The S-MP-SCOPF Var planning problem is a MINLP. A direct approach to the problem, which imposes simultaneously all constraints for all uncertainty scenarios and time periods is unmanageable by off-the-shelf solvers for a real system.

To overcome this issue, the rationale of the proposed methodology relies on the following observations regarding the structure of the Var problem. Unlike the slow, ramp rate-limited active power changes of conventional generators, the response of Var assets is quasi-instantaneous once their optimal new settings have been computed and broadcast to them. Consequently, the Var assets present no coupling constraints between successive time periods. Then, the primary coupling decision variables of the problem are the optimal size and location of the Var assets, which intervene in each tuple; a tuple (k, s, p) is a particular combination of a system state k, an uncertainty scenario s, and a time period p. Finally, the other coupling variables are, for each combination of a period and a scenario, between normal

operation and contingency state. These observations are crucial for devising a tailored efficient solution approach.

The proposed approach consists of constructing iteratively and solving a few manageable (i.e. smaller size) instances of the full original S-MP-SCOPF problem. Specifically, such an instance of the problem includes only the variables and constraints of a set of *relevant tuples* $\mathcal{T}_r = \mathcal{K}_r \times \mathcal{S}_r \times \mathcal{P}_r$, i.e. a small subset of the full set of tuples $\mathcal{K} \times \mathcal{S} \times \mathcal{P}$.

The core idea of the approach is to grow iteratively and efficiently the set of relevant tuples $\mathcal{T}_r$ until it includes the set of binding tuples, i.e. the smallest subset of the full set of tuples that leads to the same problem solution as the full set. This is achieved by combining four modules (see Fig. 1):

1) a tailored version of S-MP-SCOPF problem that computes the Var plan with discrete variables relaxed as continuous, including only the set of relevant tuples $\mathcal{T}_r$;
2) another customized version of the S-MP-SCOPF problem which calculates, for fix values of the discrete variables, if continuous variables (e.g. controllable voltages at generators, SCs, SVCs, STATCOMs) can ensure the S-MP-SCOPF problem feasibility, including only the set of relevant tuples $\mathcal{T}_r$;
3) an AC steady-state security assessment (SSSA) to unveil violated tuples $\mathcal{T}_v$, i.e. for which constraints are not met;
4) a selecion of the most critical tuples $\mathcal{T}_s \subseteq \mathcal{T}_v$ to be additionally included in the S-MP-SCOPF problem.

Fig. 1 presents the flowchart of the proposed methodology. It starts by selecting a small set of relevant tuples $\mathcal{T}_r$. Then the continuous relaxation of the S-MP-SCOPF problem is solved to calculate the Var plan including only the relevant tuples $\mathcal{T}_r$. Next, at the solution of this problem, the discrete variables are rounded off. The S-MP-SCOPF problem is solved again but with frozen discrete variables. Subsequently, the SSSA is run for the full set of tuples to detect the tuples $\mathcal{T}_v$ for which constraints are violated. The ability of preventive/corrective actions to ensure the feasibility of tuples in $\mathcal{T}_v$ is checked with the tailored AC OPF. Among the tuples that still violate constraints, one selects the most critical ones, according to the overall constraint violation metric, forming the set $\mathcal{T}_s$. The set of relevant tuples is updated $\mathcal{T}_r \leftarrow \mathcal{T}_r \cup \mathcal{T}_s$ and the iterations continue.

The aforementioned process is iteratively performed until either the SSSA or the AC OPF no longer detects any violations in terms of branch currents or voltage magnitudes for any tuple. It is intuitively expected that the methodology is able to provide a feasible solution if the posed Var problem is feasible, since the system is progressively reinforced with Var assets at each iteration as long as constraints violation are present.

In this way, the methodology determines the location, size, and type of Var sources to install.

The steps of the methodology are described in detail hereafter.

B. Input Data Generation and Collection

1) Generation of input data by post-processing the output of the reactive power scarcity break point

The proposed methodology first runs the method in [1] to identify the reactive power scarcity break point, see Fig. 1. The

Years-ahead operation during the energy transition

Input Data (for years ahead operation during the energy transition)
- Forecast load profiles
- Assume big transformations in the system (e.g., phase out of generators)
- Assume changes of RES type, installed power and location

Evaluate reactive power reserves during the energy transition

Identify the break point of reactive power scarcity

Var planning

Collect general input data:
- Load profiles
- RES production scenarios
- Network data
- Sets of $\mathcal{N}-1$ contingencies, time periods, uncertainty scenarios

Post-process output data from energy transition to identify:
- Most harmful relevant tuples $\mathcal{T}_r$
- Candidate locations for installing new Var assets

$\mathcal{T}_s = \emptyset$

$\mathcal{T}_s$

$\mathcal{T}_r \leftarrow \mathcal{T}_r \cup \mathcal{T}_s$

Filter out the non-critical tuples and select the most critical ones ($\mathcal{T}_s \subseteq \mathcal{T}_v$)

$\mathcal{T}_r$

Expand the set of Var candidate locations

Solve S-MP-SCOPF including the tuples $\mathcal{T}_r$ while treating discrete variables as continuous

Feasible? — Yes / No

Round off the discrete variables

Refine the rounding off of discrete variables

Solve S-MP-SCOPF including the tuples $\mathcal{T}_r$ with fixed discrete variables at discrete positions

Feasible? — Yes / No

Perform SSSA for all tuples combining contingencies, scenarios and time periods

Identify all violated tuples $\mathcal{T}_v$

$\mathcal{T}_v$

$\mathcal{T}_v = \emptyset$? — No / Yes

Output

Output the optimal locations, sizes and types of the new Var assets

Fig. 1: Flowchart of the proposed methodology.

output data stemming from the analysis of the break point is key to choose the initial starting point and enhance the computation performance of the proposed methodology, as follows.

First, by post-processing these data, we identify an initial small subset of candidate nodes (hot spots) for installing new Var assets. This is vital for limiting the number of (discrete) variables. The process to identify candidate nodes first computes the reactive power scarcity break point with relaxed bus voltage limits [1]. Then we rank the nodes based on their overall voltage

limit violations across all tuples. Only the nodes which are highly ranked (i.e. present the largest overall violation) are considered as potential locations for installing Var assets.

Second, as another input, the SSSA in III-D performed at the break point identifies only the most harmful tuples (with largest voltage violations), that initialize the set $\mathcal{T}_r$, limiting problem size.

2) General input data

To simulate the year's dynamics in the context of Var planning, we take into consideration the following aspects:

- a forecasted load profile with an hourly resolution for the representative days. Also, a typical yearly load increase, proportional to the peak load at each bus, is assumed;
- a RES power forecast using the *autoregressive integrated moving average* (ARIMA) [29] to define uncertainty scenarios;
- the system structure (online generators, connected lines);
- a full set of $N-1$ line contingencies.

C. S-MP-SCOPF Module and Treatment of Discrete Variables

To address rapidly discrete variables the module solves two tailored versions of the S-MP-SCOPF problem; to limit the problem size only the set of relevant tuples $\mathcal{T}_r$ are included.

The first version is the Var planning problem per se but in which the discrete variables are relaxed as continuous. After the problem is solved, the discrete variables are set by rounding off the continuous relaxed values (see Fig. 1). In particular, for Var assets, the continuous value is rounded to its nearest ceil value to avoid infeasibility due to shortage of reactive power.

The second version of the S-MP-SCOPF problem is a feasibility check. Specifically, for frozen values of the discrete variables, the problem calculates if continuous variables (i.e. controllable voltages at generators, SCs, SVCs, STATCOMs) can ensure the problem's feasibility. The objective (1) is replaced by the objective (31), which flattens the voltage profile:

$$\min_{\substack{\mathbf{P}_g, \mathbf{V}_c, \mathbf{Q}_g, \mathbf{Q}_{wp}, \mathbf{Q}_{sc}, \\ \mathbf{b}_{svc}, \mathbf{I}_{scm}}} \sum_{i,k,s,p} (V_i^{k,s,p} - 1)^2 \qquad (31)$$

Furthermore, to strengthen the voltage profile in normal operation and avoid a large number of critical tuples (a voltage violation in normal operation exacerbates under contingencies), the first iteration of the methodology does an optimal reactive power redispatch without contingencies. It solves thus a S-MP-OPF problem which optimizes (31) instead of (1).

D. SSSA Module

The SSSA relies on the full AC power flow. It computes the system response for each tuple (k, s, p), except the set of relevant tuples $\mathcal{T}_r$, at the S-MP-SCOPF solution (i.e. operating point). Thus, the module builds up the set of violated tuples $\mathcal{T}_v$, i.e. the tuples which violate limits on branch current or voltages or even lead to power flow divergence. The SSSA module acts as a pre-filter of tuples by eliminating non-critical tuples.

E. Selection of the Most Critical Tuples

The set of violated tuples $\mathcal{T}_v$ is forwarded to the tuples selector, which aims to select a small set of the most critical tuples
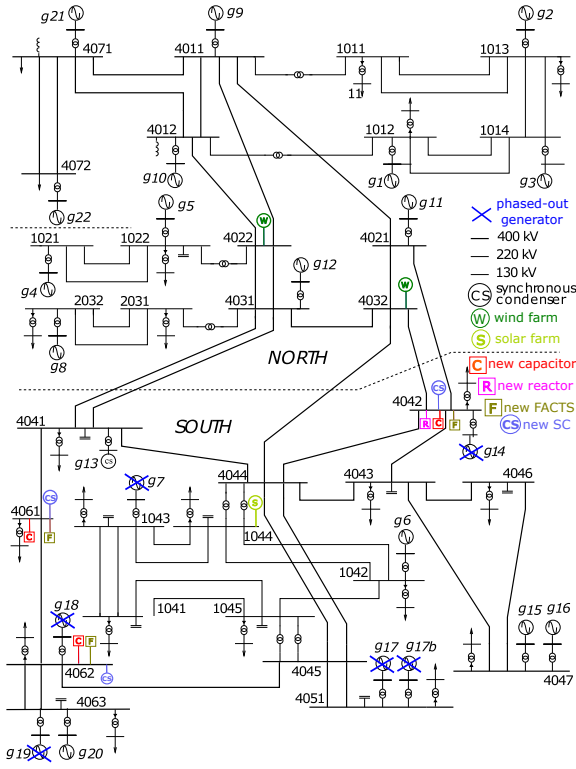
Fig. 2: One-line diagram of the modified Nordic32 system.

TABLE I: Impact of conflicting binding tuples on the objective function; $\mathcal{T}_1 = (15, 7, 12), \mathcal{T}_2 = (19, 7, 12), \mathcal{T}_3 = (21, 7, 12)$.

tuple	$\mathcal{T}_1$	$\mathcal{T}_2$	$\mathcal{T}_3$	$\mathcal{T}_1, \mathcal{T}_2$	$\mathcal{T}_1, \mathcal{T}_3$	$\mathcal{T}_2, \mathcal{T}_3$	$\mathcal{T}_1, \mathcal{T}_2, \mathcal{T}_3$
obj.	0.0	0.0	199.17	0.0	199.17	231.65	231.66

$\mathcal{T}_s$ to be further included in the S-MP-SCOPF optimization problem such that to keep manageable the problem size. To this end, the critical tuples are ranked in decreasing order of their severity measured using L_1 norm per overall overvoltages and undervoltages, respectively. A small number of top-ranked tuples are selected as the most critical ones, e.g. based on a threshold of total overvoltages and undervoltages (set here to 0.1 p.u.), and form the set $\mathcal{T}_s$.

IV. NUMERICAL RESULTS

A. Description of the Test Systems and Simulation Assumptions

This section illustrates the new features and evaluates the computational performance of the proposed methodology using two real systems: Nordic32 [2], [30] and a large one [31]. The Nordic32 system, see Fig. 2, is a model of the Swedish power system including 60 nodes and 23 generators. The large system is a modified planning version of France from the mid-90s, including 1,203 buses and 177 generators.

All simulations are conducted using the open-source Julia/JuMP programming language [32]. IPOPT solver [33] is employed to solve all S-MP-SCOPF problems. The computation times reported are obtained on a PC with an Intel i7 processor of 2.30 GHz and 48GB of RAM. The capital costs of new Var assets have been adopted from [34] and are assumed to be proportional to their sizes.

For the Nordic32 system the following changes and assumptions have been made. The planning analysis commences during the energy transition with a state that exhibits a shortage of reactive power, which is achieved by phasing out generators g17b, g18, g17, g14, g19, and g7, as elaborated in [1]. Then,

in the assumed energy transition scenario, two identical 1000-MW WPPs are deployed at nodes 4022 and 4032. Additionally, a 500-MW solar PV farm is installed at node 1044. Next, the reactive power capability of the WPPs and the reactive power limits of the conventional generators are modeled using the parameters provided in [18]. Further, for the purpose of planning, a 1-year horizon considered, which is mimicked using a selected number of representative days, with hourly resolution ($|P| = 24$). Finally, to generate realistic scenarios for WPP and solar power production, 10 scenarios ($|S| = 10$) forecasted by an ARIMA model [29], [35] have been considered.

Sections IV-B and IV-C reveal two facets of the methodology.

B. Importance of Selecting the Locations of New Var Assets

We first identify reactive power scarcity using the methodology in [1] and, as explained in section III-B1, post-process its results across contingencies and scenarios to unveil the nodes with the highest overall voltage limit violations. These nodes form the initial locations of new Var assets. For the Nordic32 system, the analysis of voltage violations pinpointed nodes 4061 and 4062 as ideal candidates for installing sources of reactive power production, and node 4042 as the preferred location for deploying sources of reactive power absorption. These locations are in the South area, which experiences a scarcity of reactive power and thereby under-voltages.

Further examination of these specific locations reveals that node 4061 offers the most cost-effective option, see the results of case#1 in Tables III and IV. Indeed, solving the Var planning problem with these three predefined locations considered simultaneously reveals that node 4061 stands out as the sole optimal choice, with an installation cost of 231.66k\$, rendering the installation of Var devices at the other two spots unnecessary. Indeed, for example, opting for node 4062 as the single capacitor installation location results in a slightly higher cost of 236.12k\$. Furthermore, for all experiments with other locations than nodes 4061 and 4062 it has been observed that the Var planning problem is infeasible as IPOPT didn't converge, declaring problem infeasibility.

These experiments clearly underline the importance of this piece of the proposed methodology, our prior work [1] serving as the foundation for the current work.

C. Revealing the Existence of Conflicting Binding Tuples

A subtle major challenge to the solution methodology of the reactive power planning problem is that many tuples (e.g. several hundred in our simulation) are going to contribute with binding (voltage) constraints at the optimum. However, only several tuples have a major impact on the objective while the other tuples have collectively a minor impact (e.g. less than 0.1%). The optimal solution calculated with the direct approach (DA) confirms this observation showing that hundreds of tuples

present minimum or maximum voltage binding constraints. However, all of them present individually small values of the corresponding Lagrange multiplier (e.g. 10^{-1} to 10^{-3}), the complementarity slackness being almost non-strict[2]. Therefore, the exact identification of binding tuples is extremely challenging by typical means (i.e. Lagrange multipliers) requiring a huge combinatorial approach.

Such observation discards the possibility of ranking tuples at any stage based on their dual variables as the tuples which influence the most of the value of the objective are not top-ranked by their dual variables. Accordingly, solving the problem to optimality is extremely difficult and not scalable as many tuples have to be included in the problem. This observation also motivates our iterative approach to reveal critical tuples iteratively and provide in a computationally scalable way a feasible and at least local optimal solution. This practical assumption can be acceptable at the planning stage.

Furthermore, higher complexity stems from the presence of conflicting tuples that we illustrate in Table I. Let $\mathcal{T}_1$, $\mathcal{T}_2$, and $\mathcal{T}_3$ be the most critical tuples, which collectively contribute to more than 90% of the optimal objective. These tuples correspond incidentally to different contingencies in the same time period and scenario; hence control actions taken in normal operation affect all contingency states. Solving the Var planning and including only one of these tuples makes a nonzero objective only for the tuple $\mathcal{T}_3$; indeed the objective value to cover tuple $\mathcal{T}_3$ is 199.17k\$, i.e. roughly 90% of the value of the optimum objective value with DA. However, as to control the low voltages for $\mathcal{T}_3$ requires deploying a capacitor bank while maximizing the usage of cost-free reactive power control means (generators' voltage and transformer ratio), the voltage profile rises, which leads to violations of the maximum bus voltage for tuples $\mathcal{T}_1$ and $\mathcal{T}_2$. In other words, the deployment and dispatch of the capacitor in normal operation for the satisfying tuple $\mathcal{T}_3$ conflicts with the constraints of initially harmless tuples $\mathcal{T}_1$ and $\mathcal{T}_2$.

However, when optimizing the three tuples together there is no need to deploy any reactor bank, but only to enhance the size of the already deployed capacitor bank, which is apparently counterintuitive. The explanation of these conflicting tuples is that the cost-free control means are able to control overvoltages but, as they cannot contribute at the same time as effectively (as in the first case) to support the undervoltages of tuple $\mathcal{T}_3$, the capacitor size is increased, raising the value of the objective.

D. Comprehensive Illustration of the Proposed Methodology

To comprehensively evaluate the problem and proposed enhancements under different conditions five test cases have been performed, where case#1 is the baseline for comparison. Table II illustrates the distinct features of these five case studies. Table III presents a comparison of the objective values and computation times obtained with both the DA, which solves the full model directly, and the proposed scalable approach. Table IV provides the needed size of new Var sources in predefined locations for each case study. Table V offers convergence details.

[2]By strict complementarity we mean that if an inequality constraint is binding its dual variable is non-zero; conversely, non-strict complementarity means that a constraint is non-binding and its dual variable is zero.

Tables III and IV indicate that the proposed approach and DA converge in all cases to the same solution (i.e. size and type of Var assets at each candidate location and accordingly the same value of the objective function), which certifies empirically the soundness of the proposed approach. Furthermore, Table III indicates that the proposed approach is much faster.

In what follows, the original problem for each case study contains 33 line contingencies ($|K| = 34$), 10 RES scenarios ($|S| = 10$), and 24 hours ($|P| = 24$) of one representative day. In addition, the initial number of contingencies, scenarios, and time periods to feed the proposed approach for all cases are the same, namely $|K_r| = 1$, $|S_r| = 10$, and $|P_r| = 24$, respectively.

1) Case#1:

Upon applying the methodology [1], bus 4042 is recommended for installing assets to absorb reactive power, while buses 4061 and 4062 are suggested for installing assets to produce reactive power. The results obtained for all cases confirm the optimality of the selected locations i.e. it is not needed to expand or alter the locations for installing new Var assets in any case. Moreover, changing these hot spots do not result in feasible solutions or reduce the investment cost.

In this case, assuming the possibility of installing static Var assets, it can be observed that both approaches provide the same solution, i.e. to install 28.96 MVar capacitors at node 4061, which demonstrates the accuracy of the proposed methodology. However, the latter is significantly faster than the DA, needing 116 s vs 2,276 s. This speed-up is due to the effectiveness of quickly identifying only 128 tuples as critical from the total of 8160 defined tuples. The large problem size reduction of roughly 62 times offers the promise of scalability.

2) Case#2:

This case highlights the importance and large impact of using refined reactive power limits for conventional generators and WPPs over the approximated constant ones. Indeed, the solution obtained consists of deploying 179.02 MVar and 13.24 MVar capacitive reactive power at nodes 4061 and 4062, respectively, i.e. much more than in case#1, which therefore underestimated the real need. Accordingly, in comparison to case#1, the investment cost considering the exact modeling of reactive power capabilities increases by 563.9% i.e., $(1538.13 - 231.66)/231.66$.

Due to the increasing complexity of the constraints, the solving time for DA and the proposed methodology rises to 207 s and 75 s, respectively. Still, the selection stage of the proposed methodology is able to identify only 141 critical tuples out of 8160, being more scalable.

3) Case#3:

Due to the quick fluctuations of power flows at high penetration of RES, the TSOs tend to favor nowadays, especially if voltage instability may be a concern, dynamic Var assets (FACTS devices including SVC and STATCOM, and synchronous condensers), which are fast reacting and have continuous control, over static Var assets, which are slow and controllable in steps. The same buses 4042, 4061, and 4062 are chosen as hot spots for these assets since all of them can produce inductive and capacitive reactive power. Note that the nodes to which these dynamic assets are connected act as controllable voltage nodes, and this constraint is imposed by (20).

TABLE II: Features of different case studies (the difference with respect to the baseline case#1 is highlighted in **bold**).

case study	case#1	case#2	case#3	case#4	case#5
type of control actions	preventive	preventive	preventive	preventive	**preventive-corrective (24)–(25)**
types of new Var asset	Q_r & Q_c	Q_r & Q_c	$\boldsymbol{Q}_{sc}$, $\boldsymbol{Q}_{svc}$ & $\boldsymbol{Q}_{scm}$	Q_r & Q_c	Q_r & Q_c
model of decision variables of new Var assets	continuous	continuous	continuous	**discrete (10 MVar stepsize)**	continuous
modelling of Q_g^{max}, Q_{wp}^{min} & Q_{wp}^{max}	constant values	**refined limits (26)–(28)**	constant values	constant values	constant values

TABLE III: Total investment cost and CPU time for the different cases.

approach	case#1	case#2	case#3	case#4	case#5
objective function (k$)					
Direct approach	231.66	1,538.13	9,323.03	240.0	0.0
S-MP-SCOPF	231.66	1,538.13	9,323.03	240.0	0.0
CPU time (s)					
Direct approach	2,276	2,484	17,596	4,091	2,321
S-MP-SCOPF	116	192	2,997	175	78

TABLE IV: Optimal location, technology, and size of new Var sources.

case study			case#1	case#2	case#3	case#4	case#5
approach	type	location	size (MVar)				
S-MP-SCOPF	r	4042	0.0	0.0	–	0.0	0.0
	c	4061	28.96	179.02	–	30.0	0.0
		4062	0.0	13.24		0.0	0.0
	sc	4042			85.34		
		4061	–	–	68.34	–	–
		4062			112.69		
	svc	4042			0.0		
		4061	–	–	0.0	–	–
		4062			0.0		
	scm	4042			0.0		
		4061	–	–	0.0	–	–
		4062			0.0		

The solution obtained consists of installing only synchronous condensers as follows: 85.34 MVar at node 4042, 68.34 MVar at node 4061, and 112.69 MVar at node 4062. These assets are favoured over SVC and STATCOM due to the lower cost for comparable performance. However, the method can accommodate operator preference at designated locations for a chosen FACTS technology e.g. based on previous experience or need. Further, in terms of computation effort, the proposed methodology obtains 83% time reduction with respect to the DA. However, compared to the other case studies, this case study requires a longer solution time due to the increasing complexity of modeling both FACTS devices and synchronous condensers concurrently as well as the highly nonlinear model of STATCOM. This case further highlights the value of our approach to accommodate a large array of Var asset technologies.

4) Case#4:

To model realistically the new Var sources, in this case, we assume that capacitors and reactors are designed to have discrete steps, with a step size of 10 MVar. As explained in section III-C, the proposed methodology uses a round-off technique applied to the continuous relaxation of discrete variables. As is evident from Table III, the investment cost for DA and the proposed methodology is the same i.e., 240.0 k$. From Table IV one can note that after the treatment of discrete variables more capacitive reactive power (i.e., 30.0 MVar) at node 4061 is needed to support voltages than in case#1. The computation time of DA is 80% larger than for the proposed methodology while the latter is still fast needing 175 s.

5) Case#5:

The results presented in Tables III to V clearly indicate that corrective controls play a crucial role in preventing the system from encountering severe instances of reactive power deficiency, thereby averting under-voltage situations or even voltage instability. The corrective controls alleviate the strain on the grid and reduce the investment in Var assets. Furthermore, it is worth noting that, due to the intricate coupling constraints, the time required by DA to achieve a feasible solution is 29 times longer than with the proposed methodology.

6) Further Technical Details of the Methodology

Table V gives further technical details of the proposed methodology, at each iteration, in terms of: objective, CPU time break-down per task, and sets of tuples violated and selected. The methodology needs between 3 and 6 iterations to discover all binding tuples. Note that the number of violated tuples has been reduced roughly by half on average, which significantly decreases the total computation time. In the worst-case (case#3) the number of tuples included in the problem has been reduced roughly only 5 times, which is due to the explained challenge to identify properly binding tuples.

E. Scalability to a Large-Scale Power System

This section ascertains the computation performance of the most computationally intense modules of the proposed methodology on the large system introduced in Section IV-A.

The planning analysis defines first an energy transition scenario and then identifies a state exhibiting severe reactive power shortage. This corresponds to displacing 19 generators by: two identical 1000 MW WPPs (at nodes 42 and 842), two identical 500 MW WPPs (at nodes 589 and 977), and two identical 500 MW solar PV farms (at nodes 1020 and 1027).

The calculation considers one representative day with hourly resolution ($|P| = 24$), three renewable generation scenarios ($|S| = 3$), and 20 pre-determined line contingencies ($|K| = 21$) prone to create voltage issues.

The results are shown in the last row of Table V. The solution consists in installing one capacitor of 5.37 MVar, rounded-off at 10 MVar, at node 28, costing 42.94k$. The solution is obtained after two outer iterations. The final S-MP-SCOPF problem includes 282 tuples and only 5 contingencies are critical and contribute to these tuples. The total solution time is below 9 hours, which is acceptable at planning stage, proving the applicability of the methodology to large, realistic cases.

Note that IPOPT fails to solve the Var problem in direct approach due to its huge size, i.e. around 5 million variables and 10 million constraints, emphasizing the necessity of taking a scalable approach as the one proposed.

case study	iter	violated tuples	additional selected tuples	obj	CPU time (s)			
					S-MP-OPF	S-MP-SCOPF	SSSA	total time
case#1	0	178	120	15.06 (p.u.)	32.22	–	0.017	
	1	55	5	225.94 (k\$)	–	23.75	0.017	
	2	3	3	231.65 (k\$)	–	29.417	0.017	116.98
	3	0	–	231.66 (k\$)	–	31.53	0.017	
case#2	0	178	120	15.06 (p.u.)	35.27	–	0.017	
	1	85	1	1,527.78 (k\$)	–	33.60	0.017	
	2	14	12	1,537.79 (k\$)	–	35.83	0.017	192.24
	3	0	–	1,538.13 (k\$)	–	87.49	0.017	
case#3	0	370	351	15.06 (p.u.)	31.14	–	0.017	
	1	285	273	7,050.32 (k\$)	–	204.20	0.017	
	2	962	821	7,658.80 (k\$)	–	270.78	0.017	
	3	163	152	9,314.02 (k\$)	–	703.82	0.017	2997.50
	4	5	1	9,323.03 (k\$)	–	793.77	0.017	
	5	0	–	9,323.03 (k\$)	–	993.69	0.017	
case#4	0	178	120	15.06 (p.u.)	32.14	–	0.017	
	1	159	3	240.0 (k\$)	–	25.63+19.46	0.017	175.65
	2	4	0	240.0 (k\$)	–	27.32+19.65	0.017	
case#5	0	178	120	15.06 (p.u.)	36.79	–	0.017	
	1	734	369	0.0 (k\$)	–	11.46	0.017	78.97
	2	0	–	0.0 (k\$)	–	30.67	0.017	
large-scale	0	273	203	84.35 (p.u.)	2,364	–		
	1	9	4	42.94 (k\$)	–	14,856	4.5	32,121
	2	0	–	42.94 (k\$)	–	14,886	4.5	

TABLE V: Further details on the numerical convergence and performance of the proposed methodology.

V. Conclusions and Future Work

The paper has proposed for the first time a framework for the Var planning problem, suitable to the ongoing energy transition to renewable-dominated generation.

First, an enhanced tailored problem formulation of Var planning has been elaborated in the form of a S-MP-SCOPF. The main enhancements of the formulation are the consideration of practical aspects such as: type of Var assets, renewable uncertainty, time of the day/year, accurate models of generators' reactive power limits, discreteness of decision variables, and corrective control. Extensive numerical results have demonstrated the important impact of each of these enhancements on the obtained solution.

Second, as the large size Var planning problem cannot be solved directly for realistic systems, a new tailored methodology, exploiting the peculiarities of the problem, has been developed. Numerical evidence on two power system models of 60 and 1203 buses, respectively, has demonstrated that the methodology achieves sufficient scalability at the planning stage in a reasonable setting. The scalability is achieved through the progressive and efficient identification of the binding combinations of contingencies, time periods, and uncertainty scenarios, which allows solving sequentially a few instances of the S-MP-SCOPF problem of much smaller size than the original problem.

The paper has revealed new insights regarding the challenges of the problem (e.g. location of new Var assets, conflicting tuples, binding tuples) and proposed effective remedies to them.

Regarding solution optimality the following remarks are notable. IPOPT is a general-purpose local solver for generic NLP problems. However, strong empirical evidence with convex relaxations techniques in the last decade showed that, in the specific field of power systems and for AC OPF or SCOPF type of problems, NLP solvers like IPOPT generally converge to the global optimum.

There are a variety of relaxations that could be developed to calculate lower bounds of the optimum and gauge the optimality of the solution calculated with our methodology. However, no relaxation provides a mathematical guarantee of its tightness i.e., how close the lower bound is to the global optimum. Accordingly, a large gap between the lower bound and the calculated solution of the methodology does not necessarily mean that the quality of the latter is not high or even the global optimum. On the other hand, if the lower bound is close to the calculated solution, it certifies the high quality of the latter. Furthermore, real-life problems are large scale (i.e. nonlinear with a few million variables and constraints) and, to our knowledge, no tight relaxation method is able to solve reliably yet such problems.

The main challenge and scaling issue of the methodology implemented pertains to the reliance on an NLP solver (e.g. IPOPT) to solve growing size instances of the S-MP-SCOPF problem, yet substantially smaller than the full problem. While the proposed methodology targets limiting the optimization problem size by the identification of binding tuples, one cannot rule out situations where, for a large system size, number of uncertainty scenarios and time periods, the size of a problem instance would exceed the capacity of IPOPT. Accordingly, the main limitation is posed by the maximum size of the NLP problem that can be solved by IPOPT on a regular computer, which amounts to a few million variables and constraints. Depending on the expected problem size, various techniques could be adapted to decompose and solve in parallel the problem across contingency states [36], time periods [37], or both [38].

Another challenge that requires further refinement is the treatment of discrete variables for large scale S-MP-SCOPF problems. The simple and fast round-off technique used in our implementation could be superseded by refined heuristic approaches that may further improve the solution optimality (e.g. progressive round-off, sensitivities, linearization) [21]–[23] at the expense of computation time increase.

The work will be further extended to consider voltage stability constraints.

References

[1] E. Davoodi, F. Capitanescu, and L. Wehenkel, "A methodology to evaluate reactive power reserves scarcity during the energy transition," *IEEE Transactions on Power Systems*, vol. 38, no. 5, pp. 4355–4368, 2022.

[2] F. Capitanescu, "Evaluating reactive power reserves scarcity during the energy transition toward 100% renewable supply," *Electric Power Systems Research*, vol. 190, p. 106672, 2021.

[3] W. Zhang, F. Li, and L. M. Tolbert, "Review of reactive power planning: objectives, constraints, and algorithms," *IEEE transactions on power systems*, vol. 22, no. 4, pp. 2177–2186, 2007.

[4] F. Capitanescu, "Are we prepared against blackouts during the energy transition?: Probabilistic risk-based decision making encompassing jointly security and resilience," *IEEE Power and Energy Magazine*, vol. 21, no. 3, pp. 77–86, 2023.

[5] K. Iba, H. Suzuki, K.-I. Suzuki, and K. Suzuki, "Practical reactive power allocation/operation planning using successive linear programming," *IEEE Transactions on Power Systems*, vol. 3, no. 2, pp. 558–566, 1988.

[6] B. Kermanshahi, K. Takahashi, and Y. Zhou, "Optimal operation and allocation of reactive power resource considering static voltage stability," in *Proceedings of POWERCON98*, vol. 2, pp. 1473–1477, IEEE, 1998.

[7] T. Van Cutsem, "A method to compute reactive power margins with respect to voltage collapse," *IEEE Trans. Pow. Syst.*, vol. 6, pp. 145–156, 1991.

[8] E. Vaahedi, Y. Mansour, C. Fuchs, S. Granville, M. D. L. Latore, and H. Hamadanizadeh, "Dynamic security constrained optimal power flow/var planning," *IEEE Trans. Pow. Syst.*, vol. 16, no. 1, pp. 38–43, 2001.

[9] C. Estevam, M. Rider, E. Amorim, and J. Mantovani, "Reactive power dispatch and planning using a non-linear branch-and-bound algorithm," *IET GTD*, vol. 4, no. 8, pp. 963–973, 2010.

[10] S. Granville and M. A. Lima, "Application of decomposition techniques to var planning: methodological and computational aspects," *IEEE transactions on power systems*, vol. 9, no. 4, pp. 1780–1787, 1994.

[11] R. A. Jabr, N. Martins, B. C. Pal, and S. Karaki, "Contingency constrained var planning using penalty successive conic programming," *IEEE Transactions on Power Systems*, vol. 27, no. 1, pp. 545–553, 2011.

[12] K. Y. Lee, X. Bai, and Y.-M. Park, "Optimization method for reactive power planning by using a modified simple genetic algorithm," *IEEE Transactions on Power Systems*, vol. 10, no. 4, pp. 1843–1850, 1995.

[13] N. Savvopoulos, C. Y. Evrenosoglu, A. Marinakis, A. Oudalov, and N. Hatziargyriou, "A long-term reactive power planning framework for transmission grids with high shares of variable renewable generation," in *2019 IEEE Milan PowerTech*, pp. 1–6, IEEE, 2019.

[14] Y. Chi, Y. Xu, and T. Ding, "Coordinated var planning for voltage stability enhancement of a wind-energy power system considering multiple resilience indices," *IEEE Transactions on Sustainable Energy*, vol. 11, no. 4, pp. 2367–2379, 2019.

[15] Y. Chi, Y. Xu, and R. Zhang, "Many-objective robust optimization for dynamic var planning to enhance voltage stability of a wind-energy power system," *IEEE Trans. Pow. Delivery*, vol. 36, no. 1, pp. 30–42, 2020.

[16] N. Gupta, "Probabilistic optimal reactive power planning with onshore and offshore wind generation, ev, and pv uncertainties," *IEEE Transactions on Industry Applications*, vol. 56, no. 4, pp. 4200–4213, 2020.

[17] A. A. Eladl, M. I. Basha, and A. A. ElDesouky, "Techno-economic multi-objective reactive power planning in integrated wind power system with improving voltage stability," *Electric Power Systems Research*, vol. 214, p. 108917, 2023.

[18] E. Davoodi, F. Capitanescu, N. Popli, and L. Wehenkel, "Re-thinking var planning to mitigate reactive power reserves scarcity during the energy transition," in *MEDPOWER, Malta (Valletta)*, IET, 2022.

[19] I. Aravena, D. K. Molzahn, S. Zhang, C. G. Petra, F. E. Curtis, S. Tu, A. Wächter, E. Wei, E. Wong, A. Gholami, *et al.*, "Recent developments in security-constrained ac optimal power flow: Overview of challenge 1 in the arpa-e grid optimization competition," *Operations research*, vol. 71, no. 6, pp. 1997–2014, 2023.

[20] J. Holzer, C. Coffrin, C. DeMarco, *et al.*, "Grid optimization competition challenge 2 problem formulation," *Technical report ARPA-E*, 2021.

[21] L. Platbrood, F. Capitanescu, C. Merckx, H. Crisciu, and L. Wehenkel, "A generic approach for solving nonlinear-discrete security-constrained optimal power flow problems in large-scale systems," *IEEE Transactions on Power Systems*, vol. 29, no. 3, pp. 1194–1203, 2013.

[22] A. Gholami, K. Sun, S. Zhang, and X. A. Sun, "An admm-based distributed optimization method for solving security-constrained alternating current optimal power flow," *Operations Research*, vol. 71, no. 6, pp. 2045–2060, 2023.

[23] C. G. Petra and I. Aravena, "A surrogate-based asynchronous decomposition technique for realistic security-constrained optimal power flow problems," *Operations Research*, vol. 71, no. 6, pp. 2015–2030, 2023.

[24] N. G. Hingorani and L. Gyugyi, "Understanding FACTS; Concepts and Technology of Flexible AC Transmission Systems," *IEEE Press*, 2000.

[25] A. Monticelli, M. Pereira, and S. Granville, "Security-constrained optimal power flow with post-contingency corrective rescheduling," *IEEE Transactions on Power Systems*, vol. 2, no. 1, pp. 175–180, 1987.

[26] F. Capitanescu and L. Wehenkel, "A new iterative approach to the corrective security-constrained optimal power flow problem," *IEEE Transactions on Power Systems*, vol. 23, no. 4, pp. 1533–1541, 2008.

[27] B. Tamimi, C. A. Canizares, and S. Vaez-Zadeh, "Effect of reactive power limit modeling on maximum system loading and active and reactive power markets," *IEEE Trans. Pow. Syst.*, vol. 25, no. 2, pp. 1106–1116, 2010.

[28] M. Sarkar, M. Altin, P. E. Sørensen, and A. D. Hansen, "Reactive power capability model of wind power plant using aggregated wind power collection system," *Energies*, vol. 12, no. 9, p. 1607, 2019.

[29] K. C. Sharma, P. Jain, and R. Bhakar, "Wind Power Scenario Generation and Reduction in Stochastic Programming Framework," *Electric Power Components and Systems*, vol. 41, no. 3, pp. 271–285, 2013.

[30] "Nordic32 system," [Online]. Available: https://github.com/MATPOWER/matpower/blob/master/data/case60nordic.m.

[31] F. Capitanescu, "Assessing Reactive Power Reserves With Respect to Operating Constraints and Voltage Stability," *IEEE Transactions on Power Systems*, vol. 26, no. 4, pp. 2224–2234, 2011.

[32] Dunning, I., Huchette, J., Lubin, M., "JuMP: A modeling language for mathematical optimization," *SIAM review*, 2017.

[33] Wächter, A., Biegler, L., Lang, Y,, Raghunathan, A., "IPOPT: An interior point algorithm for large-scale nonlinear optimization," [Online]. Available: [Online].Available:https://github.com/coin-or/Ipopt.

[34] B. Kirby and E. Hirst, "Ancillary Service Details: Voltage Control; Energy Devision," 1997.

[35] B. Singh and D. Pozo, "A guide to solar power forecasting using ARMA models," in *2019 IEEE PES ISGT-Europe*, Romania, 2019.

[36] J. Kardoš, D. Kourounis, and O. Schenk, "Two-level parallel augmented schur complement interior-point algorithms for the solution of security constrained optimal power flow problems," *IEEE Transactions on power systems*, vol. 35, no. 2, pp. 1340–1350, 2019.

[37] J. Kardoš, D. Kourounis, O. Schenk, and R. Zimmerman, "Beltistos: A robust interior point method for large-scale optimal power flow problems," *Electric power systems research*, vol. 212, p. 108613, 2022.

[38] T. Ibrahim, T. T. De Rubira, A. Del Rosso, M. Patel, S. Guggilam, and A. Mohamed, "Alternating optimization approach for voltage-secure multi-period optimal reactive power dispatch," *IEEE Transactions on Power Systems*, vol. 37, no. 5, pp. 3805–3816, 2021.